Hindawi
Journal of Sensors
Volume 2018, Article ID 9585931, 7 pages
https://doi.org/10.1155/2018/9585931

Research Article

Temperature Dependence of Dark Count Rate and After Pulsing of a Single-Photon Avalanche Diode with an Integrated Active Quenching Circuit in 0.35 μm CMOS

Michael Hofbauer, Bernhard Steindl, and Horst Zimmermann

Institute of Electrodynamics, Microwave and Circuit Engineering, TU Wien, 1040 Vienna, Austria

Correspondence should be addressed to Michael Hofbauer; michael.hofbauer@tuwien.ac.at

Received 10 April 2018; Accepted 24 May 2018; Published 2 July 2018

Academic Editor: Domenico Caputo

The temperature dependence of a single-photon avalanche diode (SPAD) with an integrated quencher in 0.35 μm CMOS is investigated. While the dark count rate strongly decreases with decreasing temperature, the after-pulsing probability (APP) does not change a lot in the investigated temperature range from −40°C to 50°C, although the dead time of the active quenching circuit (AQC) is only 9.5 ns. This and the measured histograms of the interarrival time (IAT) suggest that the traps involved have a very short lifetime, which is not strongly temperature dependent, or alternatively that the traps are not the main source of after pulses in the investigated device. Consequently, it may be necessary to find another explanation for the after pulses.

1. Introduction

Countless applications, such as fluorescence microscopy [1], distance sensing [2], data communication [3, 4], quantum cryptography [5], and positron emission tomography (PET) [6], require the capability of detecting very low amounts of light. Photo multiplier tubes (PMT) were very successful in the past, as they are capable of detecting single photons. However, compared to integrated opto-electronic detectors, they are quite bulky and expensive.

Another very successful single-photon detector is the single-photon avalanche diode (SPAD). SPADs are avalanche photo diodes (APDs) that are operated above their breakdown voltage. As soon as a photon is absorbed, the resulting electron-hole pair triggers a self-sustaining avalanche that can be measured. This avalanche needs to be stopped either by an active quenching circuit (AQC) that reduces the reverse voltage on the SPAD below the breakdown voltage or by a passive quenching circuit, typically a simple series resistor. In the passive quenching circuit, the voltage drop across the resistor reduces the reverse voltage across the SPAD below breakdown and the avalanche extinguishes.

In the period beginning with triggering the avalanche and ending with bringing the reverse voltage back to values exceeding the breakdown voltage after stopping the avalanche, the SPAD cannot detect anything. This period is called dead time.

Passive quenching circuits are typically smaller but slower (i.e., they have longer dead times) than AQCs. Since the SPAD can be implemented in CMOS as an integrated device, mass production and potentially cheap products are feasible. SPADs fabricated in optimized processes reach photon detection probabilities (PDP) of up to 75% [1]. However, SPADs suffer from some parasitic effects, of which the two most important ones result in a device-specific dark count rate (DCR) and an after-pulsing probability (APP) [7]. The dark count rate, that is, the count rate that is measured in the absence of photons, is caused by thermally generated electron-hole pairs and is typically less for purer processes. According to the literature (e.g., [7, 8]), the main source for after pulses (AP) are trapped charges that are released over time.

In this work, we investigate the temperature dependence of the dark parameters of an SPAD with an integrated active quenching circuit (AQC) in 0.35 μm CMOS. The DCR

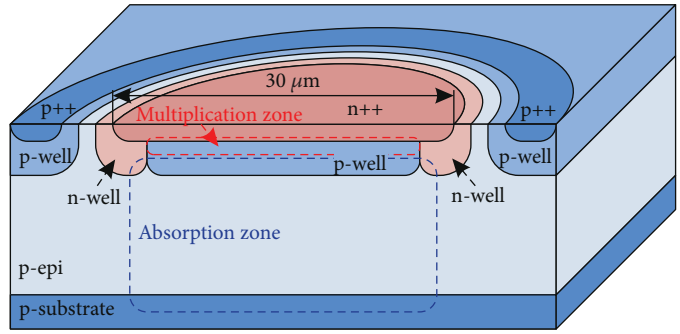

Figure 1: Cross section of the single-photon avalanche diode (SPAD) (not to scale).

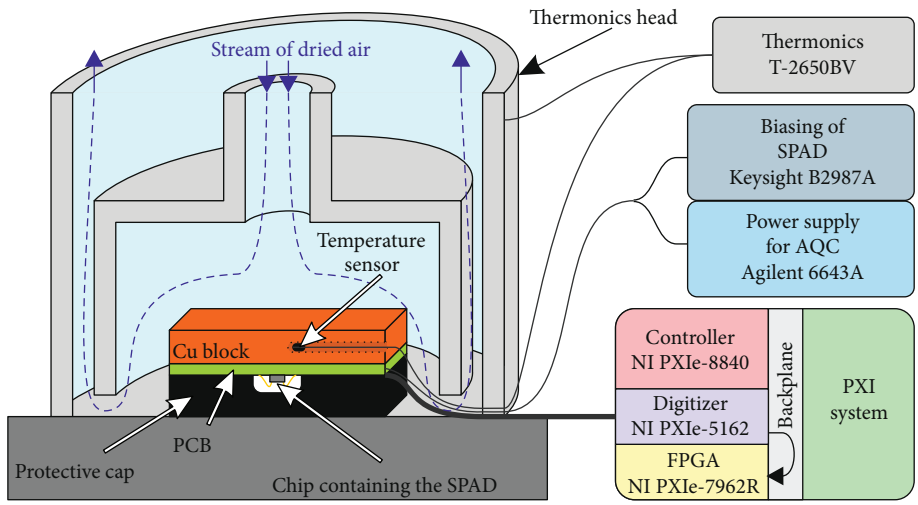

Figure 2: Measurement setup for temperature-dependent dark characterization of the SPAD.

should decrease for decreasing temperature [8], which is confirmed in our experiments, shown in the later sections. The APP should increase considerably with decreasing temperature, since the lifetime of the traps should become longer for lower temperatures. Consequently, the amount of after pluses that are triggered after the dead time of the detector should increase [7, 8]. However, in our experiments, we show that the APP increases only slightly over temperature with no evidence of significantly increased lifetimes in the interarrival times of the pulses, suggesting that another process may be the main source of the after pulses in the used technology.

2. Materials and Methods

The device under test (DUT) of this work contains a SPAD with 30 μm active diameter and an integrated active quenching circuit (AQC). The AQC is described in detail in [9]. A cross section of the SPAD is shown in Figure 1. The SPAD fabricated in pin-photodiode CMOS consists of a thick absorption zone, resulting in an improved photon detection probability (PDP) for longer wavelengths (approximately 700 nm–1000 nm) and a multiplication region formed by a p-well and a highly doped n++ region. The DCR and the APP at room temperature, as well as the wavelength dependent PDP for a SPAD in the same technology with the same layer structure, but a larger active area, are published in [10]. The dead time of the AQC is approximately 9.5 ns.

The measurement setup depicted in Figure 2 was used to characterize the dark parameters of the SPAD over temperature. The SPAD was bonded onto a PCB and protected by a protective cap, in order to prevent photons from reaching the detector. On the other side of the PCB, a copper block was mounted, which later was forced to different temperatures by the thermo-stream device Thermonics T-2650BV. This thermo-stream device streams temperated dried air to prevent condensation on the electronics. The temperature sensor of the thermo-stream device was placed in a hole inside the copper block. The temperature was swept from −40°C to +50°C in 10°C steps.

The output of the AQC was monitored by a PXI (peripheral component interconnect (PCI) extensions for instrumentation) system from National Instruments. The signals were digitized by the digitizer NI PXIe-5162 with a sampling rate of 625 MS/s. The digital values were streamed over the backplane of the PXI system to the FPGA NI PXIe-7962R that was used to extract the DCR, the APP, and the time stamps of the rising and falling edges of all the pulses. The measurement time per bias point and temperature was set to 100 s or 1 million recorded pulses whichever was reached first, in order to get a reasonable trade-off between total measurement time and measurement statistics.

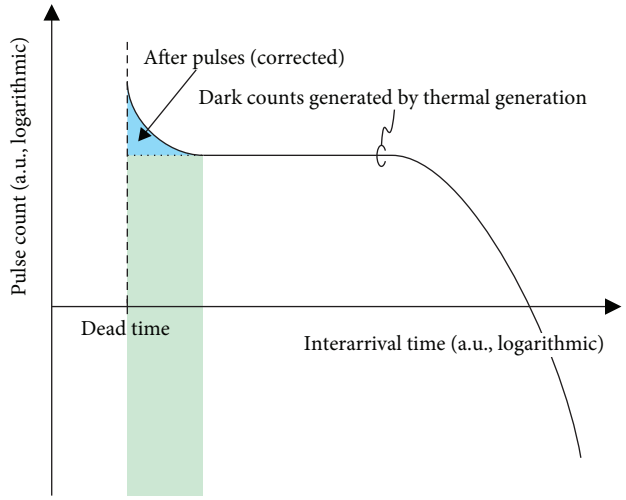

FIGURE 3: Principle of the extraction of the after-pulsing probability from the interarrival time histogram.

The dark count rate (DCR) is defined as pulses per second in dark condition (i.e., no photons entering the SPAD).

For the APP, different definitions can be found in literature. In this work, we define a pulse as after pulse if it occurs within 100 ns after another pulse. From this set of N_{AP} pulses, those that are thermally generated are subtracted. This is depictured in Figure 3. For this subtraction, the pulses received between 1 μs and 10 μs after another pulse are counted. The span from 100 ns to 1 μs is not included for the extraction of the plateau, since the interarrival time histogram is not very smooth in this range, especially for very low temperatures (see Figure 4). Since the histogram of the interarrival times (i.e., the times between two consecutive pulses) is relatively constant within the interval between 1 μs and 10 μs, this span can be used to get the average value of the constant plateau. This is done by dividing the total number of counts with interarrival times between 1 μs and 10 μs by 9 μs in order to get the height of the plateau in counts/s. This value was then multiplied by 90.5 ns (100 ns minus the dead time) in order to get the counts corresponding to a span of the plateau of 90.5 ns (i.e., the number of counts in the green rectangle in Figure 3). These thermally generated pulses are subtracted in a second step, resulting in a corrected number of after pulses $N_{AP,corr}$. This is equivalent to integrating the number of pulses in the blue area of Figure 3. In order to get the after-pulsing probability APP the corrected number of after pulses needs to be divided by the total number of measured pulses N_P.

$$\mathrm{APP} = \frac{N_{\mathrm{AP,corr}}}{N_{\mathrm{P}}} \cdot 100\% \quad (1)$$

It is evident in Figure 3 that an increased dead time can considerably decrease the after-pulsing probability. This effect was used, for example, in [11] by setting the dead time in the μs range. Please note that for our investigated device, the dead time is approximately 9.5 ns and therefore almost 3 orders of magnitude shorter.

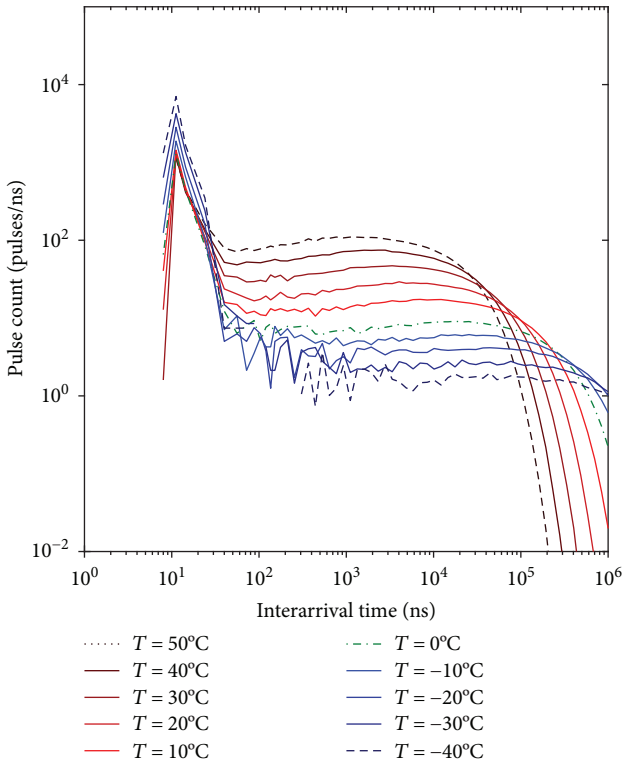

FIGURE 4: Interarrival time (IAT) histogram for different temperatures (from −40°C to 50°C) for an excess bias V_{ex} of 3.3 V (scaled for 10^6 pulses per temperature).

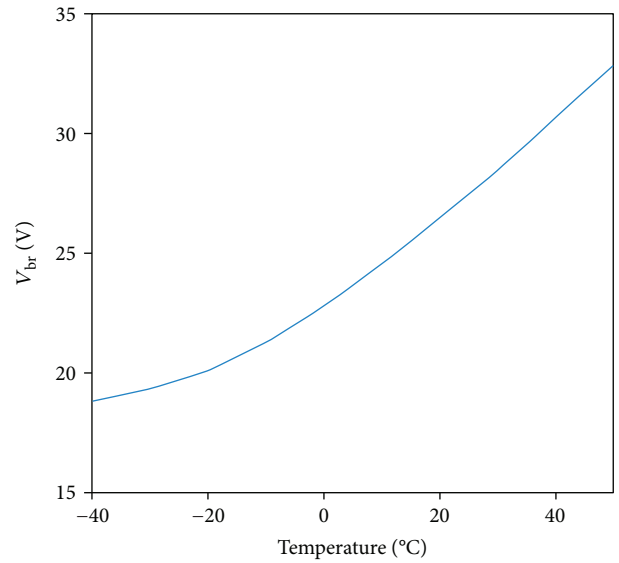

FIGURE 5: Breakdown voltage V_{br} depending on the temperature.

3. Results and Discussion

3.1. Temperature Dependence of the Breakdown Voltage. The breakdown voltage of the SPAD strongly decreases with decreasing temperature, as shown in Figure 5. The SPAD requires a reverse voltage of approximately 20 V in order to have a fully depleted p-well and a depleted absorption zone. This is important because of several reasons. If the SPAD is

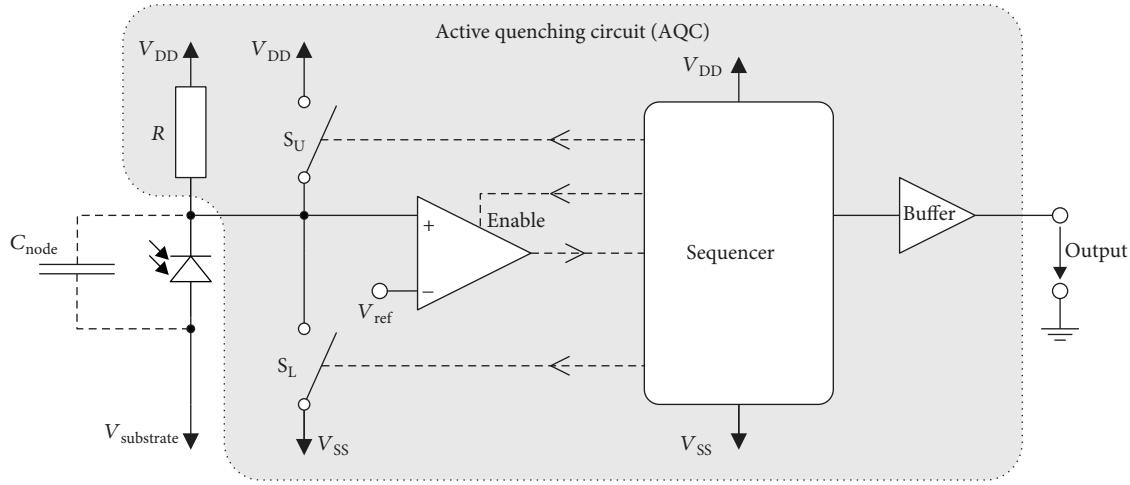

Figure 6: Simplified block diagram of the AQC.

not fully depleted, the PDP for longer wavelengths will considerably decrease. While the SPAD itself would still be operational, there are strict limitations in combination with the used AQC. If the absorption zone is not depleted, the capacitance of the SPAD is increased considerably. Since the AQC only can handle a limited capacitance of the SPAD, for a too low reverse voltage, and consequently a too large capacitance, the circuit will start oscillating and is not useable for the detection of photons anymore, before the oscillation is stopped again.

A simplified block diagram of the AQC is depicted in Figure 6 to explain why the AQC is oscillating for too large SPAD capacitances. The AQC starts quenching by closing switch S_L as soon as the differential amplifier detects that the voltage at the SPAD cathode drops below a specific threshold defined by V_{ref}. After quenching, the reverse voltage across the SPAD is set back to the value exceeding the breakdown voltage by closing the switch S_U. Additionally, after the constant dead time, the differential amplifier used for detecting voltage drops is enabled again. If the node capacitance at the SPAD cathode is too large (i.e., above ~500fF), the loading transistor cannot drive a large enough current to bring the voltage at the cathode of the SPAD to a value above the threshold before the differential amplifier is enabled again. Consequently, the AQC quenches the SPAD immediately after the differential amplifier is enabled again. Because of this, oscillations are visible at the output of the AQC.

The voltage necessary for a full depletion of the p-well and a depletion of the absorption zone is relatively constant over temperature. Consequently, by decreasing the temperature, the decreasing breakdown voltage will at some point reach the voltage necessary for full depletion. Since the AQC operates up to an excess bias of 6.6 V, there is a minimum temperature where the SPAD will still be operating.

The excess bias V_{ex} is defined as the part of the reverse voltage V_r exceeding the breakdown voltage V_{br}.

$$V_{ex} = V_r - V_{br}. \tag{2}$$

If it is required to operate SPADs with a large absorption zone at even lower temperatures, structures with higher breakdown voltages V_{br} should be used, in order to guarantee that the absorption zone is fully depleted. This is especially important for the quencher used in this work, since it is not stable anymore if the node capacitance at its input gets too large.

3.2. Temperature Dependence of the Dark Count Rate. The dark count rate (DCR) shows a strong temperature dependence. Additionally, the DCR strongly depends on the reverse voltage of the SPAD. Figure 7(a) shows the DCR over the reverse voltage at the SPAD V_r for different temperatures, while Figure 7(b) shows the DCR over the excess bias V_{ex}.

The dark count rate for an excess bias of 3.3 V decreases by approximately a factor of 1.69 per 10°C. Contrary to the results in [8], this factor for the reduction of the DCR is almost constant over the investigated temperature range. In [8], saturation effects already started at room temperature, although they had a considerably longer dead time of approximately 75 ns.

Please note that the high dark count rate at a reverse voltage V_r below 20 V can be explained by the oscillation of the AQC, since the SPAD is not fully depleted for a V_r that low.

3.3. Temperature Dependence of the Interarrival Time. In Figure 4, histograms of the interarrival time (IAT) of the measured pulses at the output of the AQC are shown for different temperatures at an excess bias V_{ex} of 3.3 V. The interarrival time is defined as the time between the leading edges of two consecutive pulses. For measuring the histograms, the measurement time was set to 100 s or 10^6 pulses, whichever was reached first. The shape of the histograms corresponds well to the expected shape. There is a quite constant plateau when using a double logarithmic scale. For very long IATs, the number of pulses decreases rapidly. The after pulses cause the increase in pulse count for very short IATs. The constant plateau decreases rapidly with decreasing temperature.

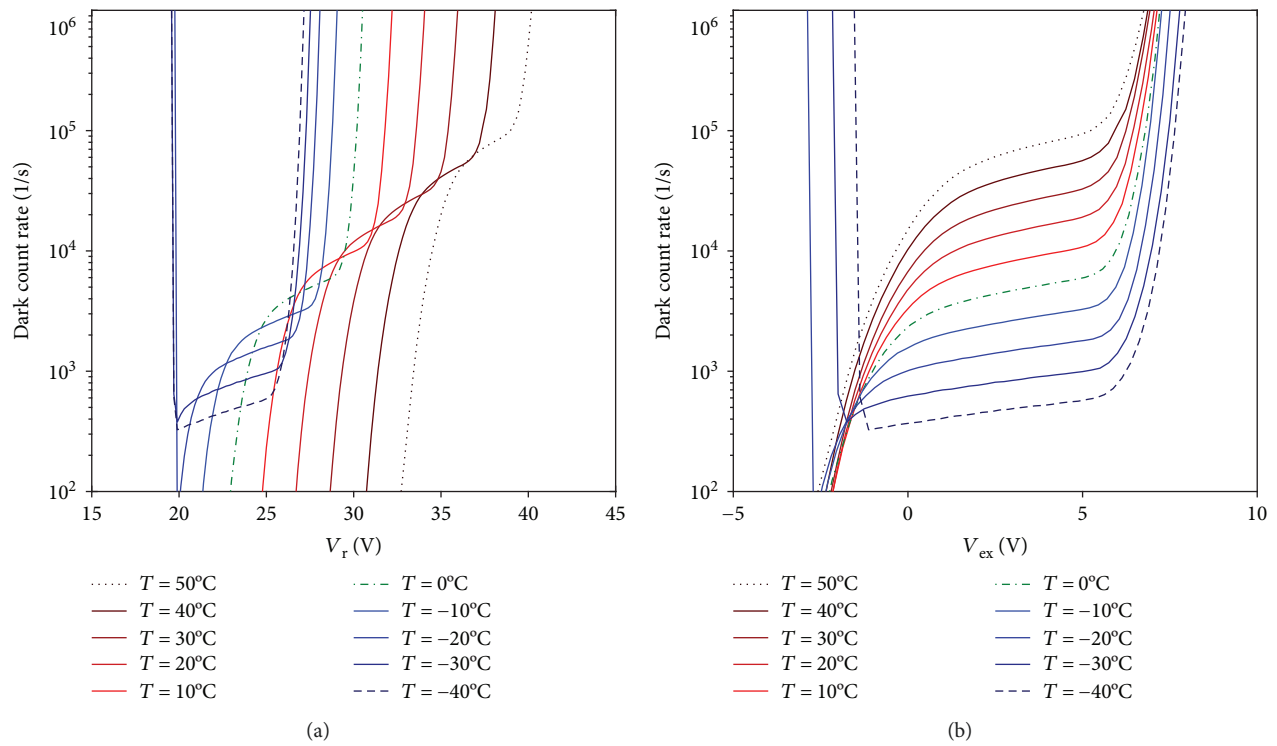

Figure 7: Dark count rate versus the reverse voltage across the SPAD V_r (a) and versus the excess bias V_{ex} (b) for different temperatures (−40°C to 50°C).

Considering the large investigated temperature range and the short dead time of the AQC, one would expect that the edge of the distribution caused by the after pulses is shifted to longer IATs for lower temperatures. While the peak of this distribution increases a bit for decreasing temperature, the edge of the distribution is not shifted to longer IATs. If traps would be the main source of after pulses, the lifetime of these traps should strongly depend on the temperature. These traps get occupied during the avalanche process. After some time, statistically characterized by the trap lifetime τ_{trap}, the charges get released. Traps that are released during the dead time of the detector will not cause an after pulse. If the temperature is decreased, according to [7], the lifetime of the traps should increase, resulting in a larger fraction of released charges after the dead time and therefore a considerable increase in after-pulsing probability. This is not visible in our measurements. Consequently, the lifetime of the traps in our device should be much shorter than the dead time and almost independent of temperature, in the investigated temperature range, or alternatively, traps may not be the main source of after pulses for the investigated technology.

Which other source can cause these after pulses? During the avalanche process, photons can be generated [12]. These photons can cause crosstalk in detector arrays. One possible explanation for the after pulses in the presented device therefore is the absorption of these generated photons outside the depleted absorption zone. If they would be absorbed within the depleted region, the generated electron-hole pair would be separated quickly. This process would be completed before the dead time of the detector ends. However, if the photon is absorbed outside the depleted region, the charge transport can be described by the much slower diffusion process. In this case, two things can happen: if the minority charge carrier recombines with a majority charge carrier, nothing will happen. But, if the minority charge carrier diffuses into the depletion region, it will be accelerated towards the multiplication region and might trigger an avalanche and therefore cause an after pulse. In [13], the diffusion time constant for an electron to diffuse over a distance of 10 μm in a similar technology is estimated to be in the range of 8 ns. Considering also the thickness of the absorption region (~12 μm), this would correspond to the characteristic absorption length of photons in the near infrared range. However, please note that the diffusion time and the diffusion length depend on many parameters such as doping concentration, the gradient of the doping concentration, the location where the photon gets absorbed, and the carrier lifetime. Therefore, further investigations are necessary.

In [14], a large number of commercial counting modules containing SPADs were investigated. Very different statistical properties of the after-pulsing distribution, even for modules of the same type, were found. The authors concluded that if the distribution of the after pulses is so different for different modules, the source for these after pulses does not lie within the physics of the SPAD but is mainly determined by the quenching circuits.

3.4. Temperature Dependence of the After-Pulsing Probability. While the breakdown voltage and the DCR strongly depend on the temperature, the after-pulsing probability of our tested device does not show such a strong dependence on temperature, as shown in Figure 8. The APP stays below

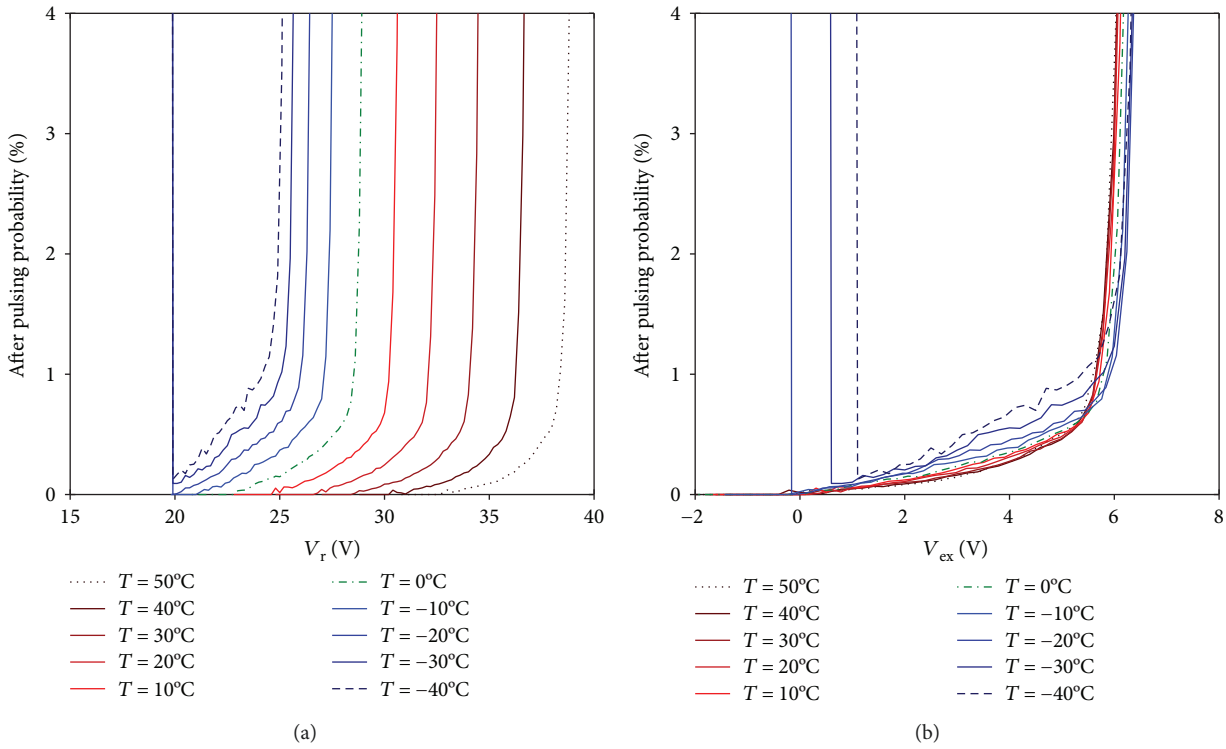

FIGURE 8: After-pulsing probability versus the reverse voltage across the SPAD V_r (a) and versus the excess bias V_{ex} (b) for different temperatures (−40°C to 50°C).

1% for a large temperature range and a large excess bias range. This result is consistent with the investigation of the interarrival times in the previous subsection. Considering the short dead time of the AQC (~9.5 ns) and the large investigated temperature range, a much larger dependence of the APP on the temperature would be expected, if traps were the main source of after pulses, as known from literature.

Consequently, as also shown in the histograms in Figure 4, trapped charges may not be the main source of after pulses in our investigated device.

4. Conclusions

In this article, we show that the investigated SPAD with an integrated active quenching circuit (AQC) in 0.35 μm CMOS does not show a strong temperature dependence of the after-pulsing probability in the temperature range between −40°C and 50°C. Consequently, traps commonly expected to be the main source of after pulses in SPADs may not be the main source of after pulses for the investigated device, since the lifetime of such traps typically is strongly temperature dependent. This result shows that it is feasible to use cooling in the given technology and SPAD structure to reduce the dark count rate (DCR) without strong influence on the after-pulsing probability (APP), even for very short dead times in the range of 10 ns. Photons emitted during the avalanche process, generating electron-hole pairs in the substrate, of which electrons diffuse up into the depleted absorption zone, are potential candidates to explain this behaviour, which will be further investigated in the future.

Data Availability

All data used for the results presented within the article can be accessed upon request by contacting the authors.

Conflicts of Interest

The authors declare that there is no conflict of interest regarding the publication of this paper.

Acknowledgments

The authors acknowledge financial support from the Austrian Science Fund (FWF) under Grant no. P28335-N30. The authors would like to thank Kevin Pail for bonding the chips onto the printed circuit boards (PCBs).

References

[1] X. Michalet, A. Ingargiola, R. A. Colyer et al., "Silicon photon-counting avalanche diodes for single-molecule fluorescence spectroscopy," *IEEE Journal of Selected Topics in Quantum Electronics*, vol. 20, no. 6, article 3804420, pp. 248–267, 2014.

[2] F. Villa, B. Markovic, S. Bellisai et al., "SPAD smart pixel for time-of-flight and time-correlated single-photon counting measurements," *IEEE Photonics Journal*, vol. 4, no. 3, pp. 795–804, 2012.

[3] B. Steindl, M. Hofbauer, K. Schneider-Hornstein, P. Brandl, and H. Zimmermann, "Single-photon avalanche photodiode based fiber optic receiver for up to 200 Mb/s," *IEEE Journal*

of Selected Topics in Quantum Electronics, vol. 24, no. 2, article 3801308, pp. 1–8, 2018.

[4] B. Goll, M. Hofbauer, B. Steindl, and H. Zimmermann, "A fully integrated SPAD-based CMOS data-receiver with a sensitivity of −64 dBm at 20 Mb/s," *IEEE Solid-State Circuits Letters*, vol. 1, no. 1, pp. 2–5, 2018.

[5] R. H. Hadfield, "Single-photon detectors for optical quantum information applications," *Nature Photonics*, vol. 3, no. 12, pp. 696–705, 2009.

[6] F. Powolny, E. Auffray, S. E. Brunner et al., "Time-based readout of a silicon photomultiplier (SiPM) for time of flight positron emission tomography (TOF-PET)," *IEEE Transactions on Nuclear Science*, vol. 58, no. 3, pp. 597–604, 2011.

[7] M. Stipcevic, D. Wang, and R. Ursin, "Characterization of a commercially available large area, high detection efficiency single-photon avalanche diode," *Journal of Lightwave Technology*, vol. 31, no. 23, pp. 3591–3596, 2013.

[8] A. Rochas, M. Gani, B. Furrer et al., "Single photon detector fabricated in a complementary metal–oxide–semiconductor high-voltage technology," *Review of Scientific Instruments*, vol. 74, no. 7, pp. 3263–3270, 2003.

[9] R. Enne, B. Steindl, M. Hofbauer, and H. Zimmermann, "Fast cascoded quenching circuit for decreasing afterpulsing effects in 0.35- μ m CMOS," *IEEE Solid-State Circuits Letters*, vol. 1, no. 3, pp. 62–65, 2018.

[10] H. Zimmermann, B. Steindl, M. Hofbauer, and R. Enne, "Integrated fiber optical receiver reducing the gap to the quantum limit," *Scientific Reports*, vol. 7, no. 1, p. 2652, 2017.

[11] I. Rech, I. Labanca, G. Armellini, A. Gulinatti, M. Ghioni, and S. Cova, "Operation of silicon single photon avalanche diodes at cryogenic temperature," *Review of Scientific Instruments*, vol. 78, no. 6, article 063105, 2007.

[12] I. Rech, A. Ingargiola, R. Spinelli et al., "A new approach to optical crosstalk modeling in single-photon avalanche diodes," *IEEE Photonics Technology Letters*, vol. 20, no. 5, pp. 330–332, 2008.

[13] H. K. Zimmermann, *Integrated Silicon Optoelectronics*, Springer, Berlin, Heidelberg, 2010.

[14] A. W. Ziarkash, S. K. Joshi, M. Stipčević, and R. Ursin, "Comparative study of afterpulsing behavior and models in single photon counting avalanche photo diode detectors," *Scientific Reports*, vol. 8, no. 1, p. 5076, 2018.